Neuron
Report

Accelerated Experience-Dependent Pruning of Cortical Synapses in *Ephrin-A2* Knockout Mice

Xinzhu Yu,[1] Gordon Wang,[2] Anthony Gilmore,[1] Ada Xin Yee,[3] Xiang Li,[4] Tonghui Xu,[1] Stephen J. Smith,[2] Lu Chen,[3] and Yi Zuo[1,*]
[1]Department of Molecular Cell and Developmental Biology, University of California, Santa Cruz, Santa Cruz, CA 95064, USA
[2]Department of Molecular and Cellular Physiology
[3]Department of Psychiatry and Behavioral Science
Stanford University, Stanford, CA 94305, USA
[4]Department of Neuroscience, Columbia University, New York, NY 10032, USA
*Correspondence: yizuo@ucsc.edu
http://dx.doi.org/10.1016/j.neuron.2013.07.014

SUMMARY

Refinement of mammalian neural circuits involves substantial experience-dependent synapse elimination. Using in vivo two-photon imaging, we found that experience-dependent elimination of postsynaptic dendritic spines in the cortex was accelerated in *ephrin-A2* knockout (KO) mice, resulting in fewer adolescent spines integrated into adult circuits. Such increased spine removal in *ephrin-A2* KOs depended on activation of glutamate receptors, as blockade of the *N*-methyl-D-aspartate (NMDA) receptors eliminated the difference in spine loss between wild-type and KO mice. We also showed that ephrin-A2 in the cortex colocalized with glial glutamate transporters, which were significantly downregulated in *ephrin-A2* KOs. Consistently, glial glutamate transport was reduced in *ephrin-A2* KOs, resulting in an accumulation of synaptic glutamate. Finally, inhibition of glial glutamate uptake promoted spine elimination in wild-type mice, resembling the phenotype of *ephrin-A2* KOs. Together, our results suggest that ephrin-A2 regulates experience-dependent, NMDA receptor-mediated synaptic pruning through glial glutamate transport during maturation of the mouse cortex.

INTRODUCTION

Postnatal experience-dependent synapse elimination is crucial for the establishment of properly connected neuronal circuits in the mature brain. Synapse elimination prunes the supernumerary imprecise connections formed during the initial overproduction of synapses, while strengthening functionally important connections (Changeux and Danchin, 1976; Hubel et al., 1977; Katz and Shatz, 1996; Lichtman and Colman, 2000). The majority of excitatory glutamatergic synapses in the mammalian brain reside at dendritic spines, which contain all necessary postsynaptic signaling machinery and serve as a good proxy for synaptic connectivity (Nimchinsky et al., 2002; Segal, 2005; Tada and Sheng, 2006; Yuste and Bonhoeffer, 2001). Recent in vivo two-photon imaging studies have shown that dendritic spines of cortical pyramidal neurons across various cortical regions undergo rapid elimination during adolescent development. In the adult brain, spine elimination continues at a much lower rate, and spines surviving the pruning process build the foundation of the mature circuits (Holtmaat et al., 2005; Yang et al., 2009; Zuo et al., 2005a, 2005b). Although experience- or activity-dependent plasticity is believed to drive the extensive and prolonged synaptic pruning, the molecular mechanisms underlying this process remain largely unknown.

Ephrins and their Eph receptors are attractive candidates for modulating structural plasticity of synapses, because of their synaptic expression and ability to coordinate contact-mediated bidirectional signaling in ligand- and receptor-containing cells (Aoto and Chen, 2007; Klein, 2009; Lai and Ip, 2009; Murai and Pasquale, 2004). Based on their cell membrane attachment and binding preference to Eph receptors, ephrins are classified into two groups: (1) GPI-linked ephrin-As that preferentially interact with EphA receptors and (2) transmembrane ephrin-Bs that preferentially bind to EphB receptors. While it is generally believed that ephrin-Bs and EphB receptors act through transsynaptic interactions to modulate synapse development and plasticity, ephrin-As and EphA receptors have been shown to mediate astrocyte-neuron interactions at mature hippocampal synapses. In particular, ephrin-A3 ligands are expressed in astrocytic processes, and EphA4 receptors are localized to postsynaptic spines of CA1 pyramidal neurons (Murai et al., 2003). In cultured hippocampal slices, while activation of EphA4 receptors by ephrin-A3 ligands induces spine retraction, disruption of this interaction leads to elongation of spine length (Murai et al., 2003). However, the roles of ephrin-As in experience-dependent synaptic pruning remain unknown.

In this study, we show that elimination of dendritic spines from cortical pyramidal neurons is greatly enhanced in *ephrin-A2*, but not *ephrin-A3*, knockout (KO) mice during adolescent development, through an experience-dependent, NMDA receptor-mediated mechanism. The imbalance between spine formation and elimination leads to an accelerated reduction in the number of total spines in adult mice. We also find that glial glutamate transporters (GLAST and GLT-1) are closely associated with ephrin-A2 proteins. The expression of glial glutamate transporters is downregulated in *ephrin-A2* KOs, resulting in decreased glial

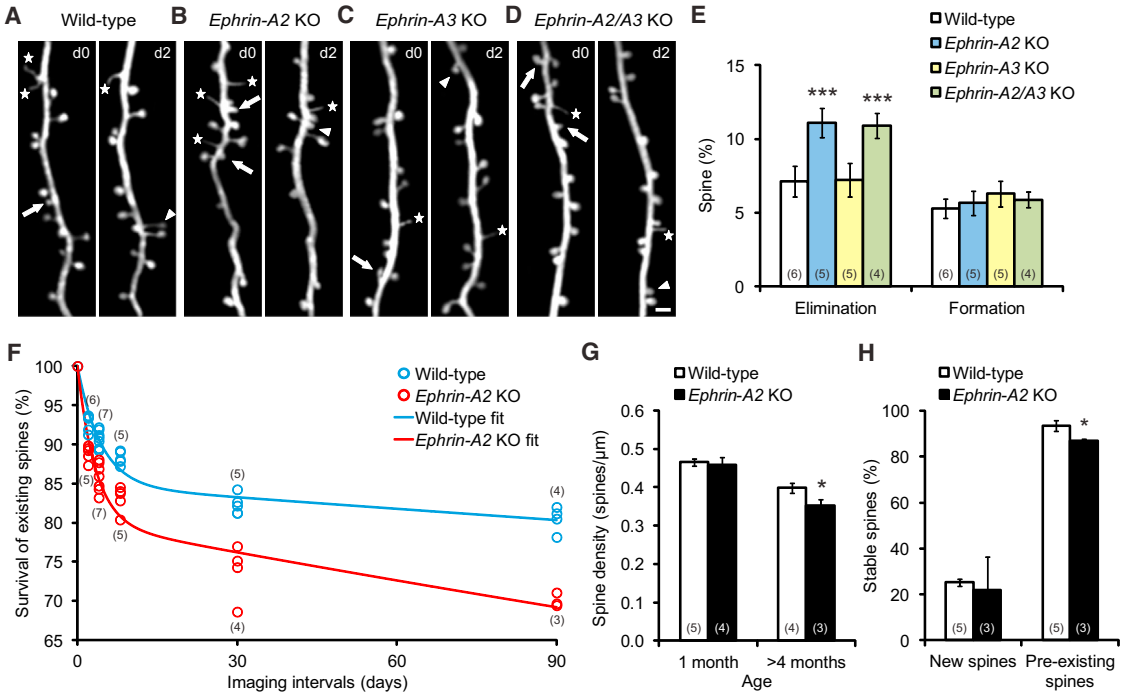

Figure 1. Dendritic Spine Elimination, but Not Formation, Is Significantly Increased in 1-Month-Old *Ephrin-A2* KOs

(A–D) Repeated imaging of the same dendritic branches over 2-day intervals in the motor cortex reveals spine elimination (arrows) and formation (arrowheads), as well as filopodia (stars), in wild-type (A), *ephrin-A2* KO (B), *ephrin-A3* KO (C), and *ephrin-A2/A3* KO (D) mice. Scale bar represents 2 μm.

(E) Percentages of spines eliminated and formed over 2 days in the motor cortex of wild-type and KO mice.

(F) Percentages of spines that survived over 2, 4, 8, 30, and 90 days in wild-type and *ephrin-A2* KO mice. Data were fitted by two-phase exponential decay equations.

(G) Spine density of layer V neuron apical dendrites in wild-type and *ephrin-A2* KO mice in adolescence and adulthood.

(H) Survival percentages of new and pre-existing spines over 4 days in wild-type and *ephrin-A2* KO mice.

Data are presented as mean ± SD. *$p < 0.05$, ***$p < 0.001$. See also Figures S1 and S2.

glutamate uptake and increased synaptic glutamate level. Finally, pharmacological inhibition of glial glutamate uptake promotes spine elimination in the cortex of wild-type mice.

RESULTS

Ephrin-A2 KO Mice Have Elevated Spine Elimination in the Cortex during Adolescent Development

To investigate whether and how ephrin-As affect synapse development, we crossed *ephrin-A2* or *ephrin-A3* single and double KO mice with YFP-H line mice, which express cytoplasmic yellow fluorescent protein (YFP) predominantly in a subpopulation of layer V cortical neurons (Feng et al., 2000). We did not find any difference in cortical organizations or spine density along apical dendrites in layer V neurons between *ephrin-A2/A3* KO and wild-type mice at 1 month of age (Figure S1 available online). To determine whether spine dynamics were affected in *ephrin-A* KOs, we repeatedly imaged apical dendritic branches and followed spine dynamics in the motor cortex by transcranial two-photon microscopy. We found that, while the amount of new spines added over 2 days was comparable between *ephrin-A2* KOs and their wild-type littermates, significantly more spines were eliminated during the same period of time in KOs (Figures 1A, 1B, and 1E; $p < 0.001$). Unlike *ephrin-A2* KOs, *ephrin-A3* KOs exhibited similar spine turnover to wild-type controls (Figures 1C and 1E; $p > 0.1$). In addition, spine elimination in *ephrin-A2/A3* double KOs was comparable to that of *ephrin-A2* single KOs (Figures 1D and 1E; $p > 0.7$). Moreover, we found that the increase in spine elimination occurred in various cortical regions of *ephrin-A2* KOs (Figure S2) and persisted over prolonged imaging intervals (Figure 1F). As a consequence, despite the normal spine density at 1 month of age ($p > 0.2$), spine density of adult *ephrin-A2* KOs was lower than that of wild-type mice (Figure 1G; $p < 0.05$). Thus, developmentally regulated spine pruning is accelerated in *ephrin-A2* KOs.

Fewer Adolescent Spines Are Incorporated into the Adult Neural Circuits in *Ephrin-A2* KO Mice

Spines formed during early development and surviving extensive pruning have greatly contributed to stably connected neural networks in adulthood (Yang et al., 2009; Zuo et al., 2005a). To investigate how accelerated spine elimination during adolescent development influences adult synaptic connections in *ephrin-A2* KOs, we calculated the lifetime of dendritic spines in both wild-type and *ephrin-A2* KO mice, based on spine elimination measured over various imaging intervals (i.e., 2, 4, 8, 30, and 90 days), starting at 1 month of age (Figure 1F). We found that the spine survival curve of wild-type mice was well fitted by a

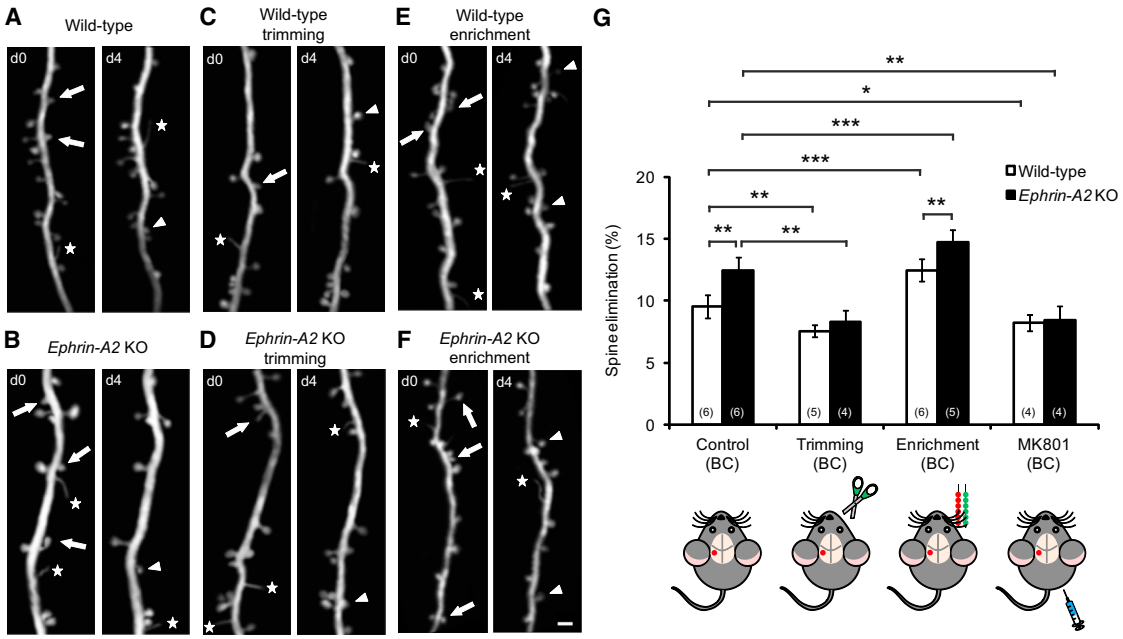

Figure 2. Sensory Experience Is Necessary for Elevated Spine Elimination in *Ephrin-A2* KOs

(A–F) Repeated imaging of the same dendritic branches over 4 days in the barrel cortex of wild-type and *ephrin-A2* KO mice under control (A and B), deprived (C and D), and sensory-enriched (E and F) conditions. Scale bar represents 2 μm.

(G) Percentages of spines eliminated over 4 days in the barrel cortex (BC) under different conditions.

Data are presented as mean ± SD. *p < 0.05, **p < 0.01, ***p < 0.001. See also Figure S3.

two-phase exponential decay equation (R^2 = 0.92, see Experimental Procedures), with a small portion of spines rapidly lost ("fast-decay spines," 15%, half-life 3.0 days) and the rest stable over months ("slow-decay spines," half-life 1,112 days). Fitting the spine survival curve of *ephrin-A2* KOs with the same formula (R^2 = 0.90), we found that while the half-life of the fast-decay spine population in KOs was comparable to that of wild-type mice (2.3 days, p > 0.4), the half-life of the slow-decay spine population was significantly shorter in KOs (432 days, p < 0.01). As previous studies have revealed that newly formed spines are much more vulnerable to elimination than pre-existing spines (Xu et al., 2009; Yang et al., 2009), the fast- and slow-decay spines could represent new and pre-existing spines, respectively. To determine whether the survival of new and pre-existing spines was, indeed, affected differently in *ephrin-A2* KOs, we imaged the same mice three times (i.e., day 0, 1, and 5), identified new spines and pre-existing spines based on their appearance in the first two images, and quantified their survival rates using the last images. Indeed, while the survival rate of new spines was comparable between *ephrin-A2* KO and wild-type mice (p > 0.5), the survival rate of pre-existing spines was significantly lower in *ephrin-A2* KOs (Figure 1H; p < 0.05). Such results agree with the lifetime analysis, suggesting a selective but long-lasting effect of ephrin-A2 on the removal of stable spines.

Sensory Experience Is Required for Elevated Spine Elimination in the Barrel Cortex of Adolescent *Ephrin-A2* KO Mice

Experience drives synapse elimination during postnatal development. We found that deprivation of sensory experience by unilateral whisker trimming at 1 month of age significantly reduced spine elimination in the contralateral barrel cortex of both wild-type and *ephrin-A2* KO mice (Figures 2A–2D and 2G; p < 0.005). In contrast, spine formation was unaffected by whisker trimming over the same period (Figure S3). Furthermore, there was no difference in spine elimination between deprived wild-type and deprived KO mice (p > 0.2), suggesting that sensory experience is necessary for elevated spine elimination in *ephrin-A2* KOs.

In contrast to sensory deprivation, different environmental enrichment (EE) protocols have been shown to promote both spine elimination and spine formation in various cortical areas of living mice (Fu et al., 2012; Yang et al., 2009). Using a sensory EE paradigm, we found that spine elimination in the barrel, but not the motor, cortex of both wild-type and KO mice was robustly increased, and significantly more spines were removed in KOs compared with wild-type mice under sensory EE (Figures 2E–2G and S3; p < 0.005). In addition, sensory EE promoted spine formation to comparable high levels in wild-type and KO mice (Figure S3). Together, these results indicate that lack of ephrin-A2 selectively affects experience-dependent spine loss but not experience-dependent spine growth.

NMDA Receptors Mediate Elevated Spine Elimination in *Ephrin-A2* KO Mice

Many lines of evidence have shown that NMDA receptor activation is essential for synaptic plasticity in various systems (Bock and Braun, 1999; Nicoll and Malenka, 1999; Sawtell et al., 2003; Sin et al., 2002). We found that, in the barrel cortex, blockade of NMDA receptors affected spine elimination in a

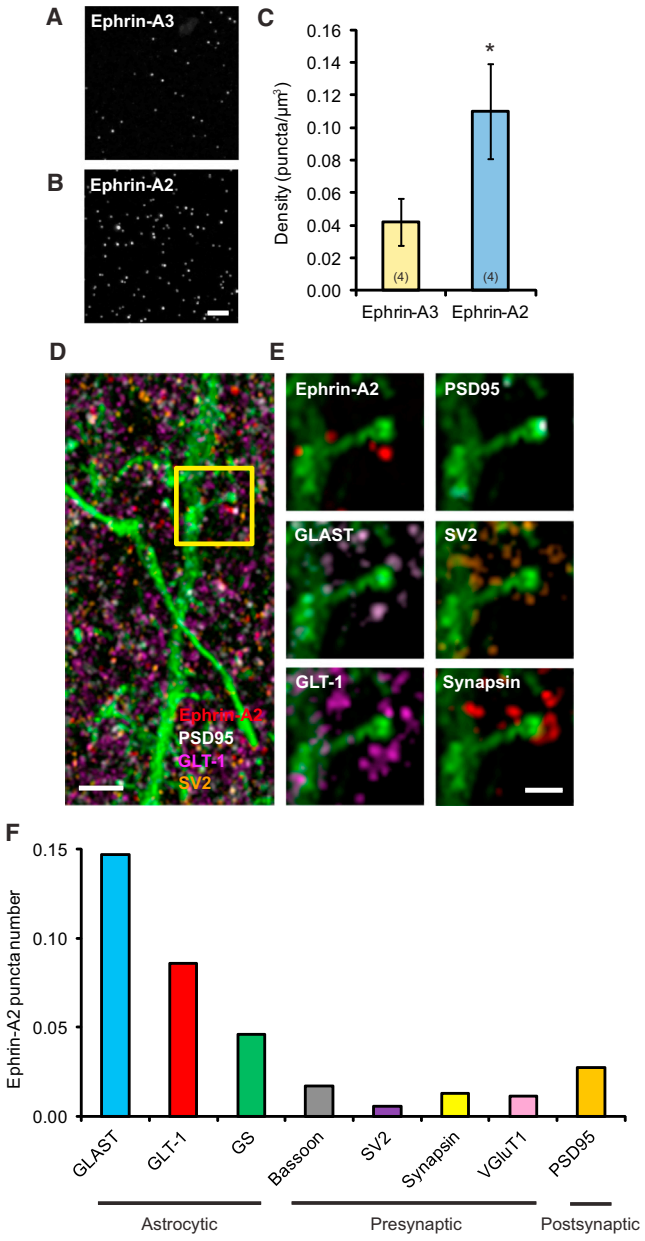

Figure 3. Ephrin-A2 Colocalizes with Astrocytic Glutamate Transporters in the Mouse Cortex

(A and B) Representative image volumes of ephrin-A2 and ephrin-A3 immunofluorescence staining in superficial layer I of 1-month-old mouse cortex. Each image is a maxium projection of five serial sections. Scale bar represents 10 μm. Data are presented as mean ± SEM. *$p < 0.05$.

(C) Quantification of puncta density shows that ephrin-A2 is approximately three times enriched, compared to ephrin-A3 in the cortex.

(D) Maximum projection of 36 serial sections of ephrin-A2 immunofluorescence (red) with protein markers of presynaptic SV2 (orange), postsynaptic PSD95 (white), astrocytic GLT-1 (magenta), and dendritic segment labeled with YFP (green). Scale bar represents 1 μm.

(E) Images of a spine from the boxed region in (D) at higher magnification with various protein markers. Scale bar represents 500 nm.

(F) Average numbers of ephrin-A2 puncta within 100 nm from the centers of different neuronal and astrocytic constituents.

See also Figure S4.

fashion similar to that of sensory deprivation. Four-day treatment with MK801, a selective antagonist of NMDA receptors, significantly decreased spine elimination in both wild-type and *ephrin-A2* KO mice (Figure 2G; $p < 0.05$), without affecting spine formation (Figure S3). MK801 treatment also eliminated the differences in spine loss between wild-type and KO mice ($p > 0.7$), suggesting that elevated spine elimination in *ephrin-A2* KOs is mediated by NMDA receptors.

Ephrin-A2 Colocalizes with Glial Glutamate Transporters in the Mouse Cortex

The expression of both ephrin-A2 and ephrin-A3 mRNAs in embryonic and adult mouse cortices is well documented (Cang et al., 2005; Murai et al., 2003; Torii et al., 2009). A transcriptome database has reported cell-type-specific expression profiles of ephrin-A2 and ephrin-A3 in the mouse forebrain: while ephrin-A2 mRNAs are enriched in astrocytes, ephrin-A3 mRNAs are enriched in neurons (Cahoy et al., 2008). However, little is known about the cortical expression of their protein products. To address this question, we took advantage of array tomography (AT), a proteomic imaging method that offers the ability to resolve individual synapses and analyze their protein profiles at ultrastructural level (Micheva et al., 2010; Micheva and Smith, 2007). As illustrated in Figures 3A and 3B, individual ephrin-A2 and ephrin-A3 puncta were clearly resolved using AT from cortical sections of adolescent wild-type mice, but not *ephrin-A2/A3* KOs (Figure S4). The densities of ephrin-A2 and ephrin-A3 puncta were relatively consistent throughout all cortical layers (Figure S4). Subsequent quantitative analyses further revealed that the density of ephrin-A2 puncta was approximately three times the density of ephrin-A3 puncta in the superficial cortical layers (Figure 3C).

To further investigate the subcellular localizations of ephrin-As near cortical synapses, we colabeled ephrin-A2 and ephrin-A3 proteins with different synaptic (presynaptic: bassoon, synapsin, VGluT1, and SV2; postsynaptic: PSD95) and astrocytic (GLAST, GLT-1, and GS) markers (Figures 3D and 3E) and then analyzed the spatial distribution of ephrin-As around different protein constituents in three dimensions at excitatory synapses. Our analyses revealed that the numbers of ephrin-A2 puncta within 100 nm from the centers of astrocytic proteins, especially GLAST and GLT-1, were higher than those around neuronal synaptic markers (Figure 3F), whereas ephrin-A3 puncta were more aligned to presynaptic markers (Figure S4). Membrane-bound glial glutamate transporters, GLAST and GLT-1, are enriched in perisynaptic astrocytic processes and associated tightly with excitatory synapses (Chaudhry et al., 1995). Thus, in agreement with the transcriptome data, our results show that while ephrin-A3 is predominantly presynaptic, ephrin-A2 localizes predominantly to astrocytic processes near synapses.

Glial Glutamate Transporters Are Downregulated in *Ephrin-A2* KO Mice

Having shown that ephrin-A2 colocalized with glial glutamate transporters, we next examined whether cortical expression of glial glutamate transporters was altered in *ephrin-A2* KOs. While the density, size, and morphology of cortical astrocytes were indistinguishable between wild-type and *ephrin-A2* KO mice

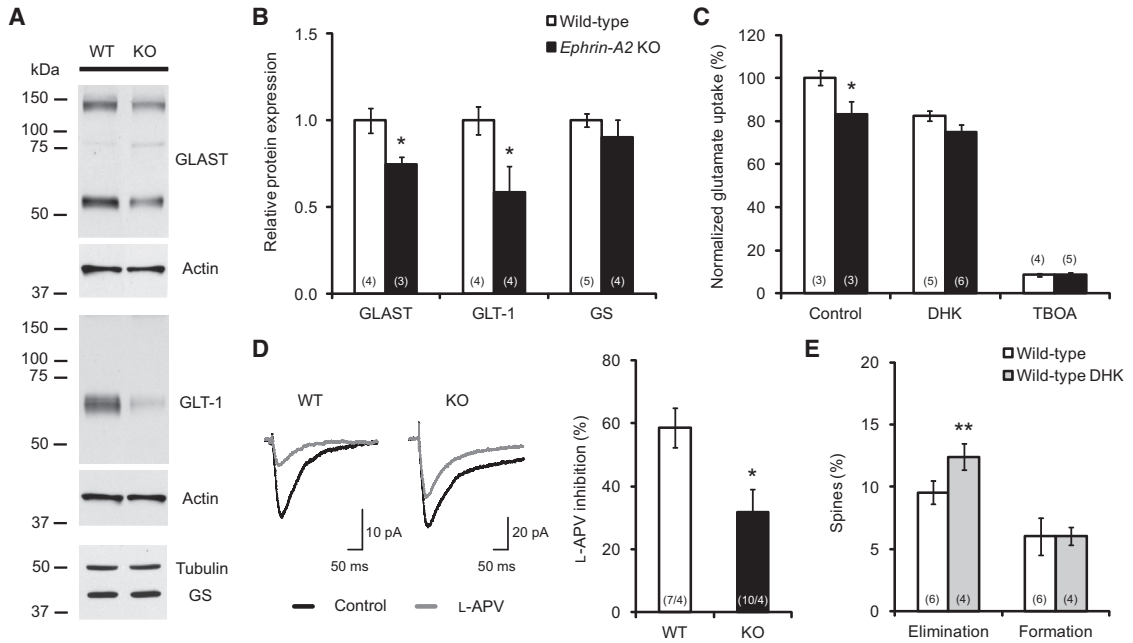

Figure 4. Glial Glutamate Transporters Are Downregulated in *Ephrin-A2* KOs

(A and B) Western blot examples (A) and quantification (B) reveal a downregulation of glial glutamate transporters in the cortex of KO mice.

(C) Normalized glutamate uptake efficiencies in cortical slices of 1-month-old wild-type and KO mice, with and without glial glutamate transporter inhibitors (DHK and TFB-TBOA).

(D) L-APV inhibition of eEPSCs is significantly reduced in KO cortical slices compared with wild-type slices.

(E) Percentages of spines eliminated over 4 days in wild-type mice with and without DHK treatment.

Data are presented as mean ± SEM. *$p < 0.05$, **$p < 0.01$. See also Figure S5.

(Figure S5), cortical expression levels of GLAST and GLT-1 were significantly decreased compared with wild-type controls (Figures 4A, 4B, and S5). Specifically, there was about 25% reduction of GLAST ($p < 0.05$) and about 40% reduction of GLT-1 ($p < 0.05$) in *ephrin-A2* KOs. In contrast, the expression of GS, another astrocytic enzyme involved in glutamate recycling (Hertz and Zielke, 2004), remained unaltered in *ephrin-A2* KOs (Figures 4A and 4B; $p > 0.4$). Further analysis of mRNA expression of GLAST and GLT-1 revealed a comparable level between wild-type and *ephrin-A2* KO mice (Figure S5), suggesting that downregulation of GLAST and GLT-1 occurs at the posttranscriptional level in *ephrin-A2* KOs. Moreover, a decreasing trend in the expression of glial glutamate transporters was found in the contralateral barrel cortex following whisker trimming in both wild-type and KO mice (Figure S5), indicating an experience-dependent modulation of glial glutamate uptake.

Glial Glutamate Transport Is Reduced and Synaptic Glutamate Level Is Elevated in *Ephrin-A2* KO Mice

Membrane-bound glial glutamate transporters uptake glutamate from the synaptic cleft to regulate synaptic transmission (Tzingounis and Wadiche, 2007). We next investigated whether glutamate transport was affected in *ephrin-A2* KO mice, using radioactive tracer L-[^{3}H]-glutamate on cortical slices of 1-month-old mice. We found that the efficiency of glutamate uptake was reduced by about 17% in *ephrin-A2* KOs compared with wild-type mice (Figure 4C; $p < 0.05$). Moreover, in the presence of high-affinity blocker of glial glutamate transporters, (3*S*)-3-[[3-[[4-(trifluoromethyl)benzoyl]amino]phenyl]methoxy]-L-aspartic acid (TFB-TBOA), glutamate uptake was decreased to comparable low levels in wild-type and KO cortical slices (Figure 4C), suggesting that reduced glutamate uptake is mostly due to decreased functions of glial glutamate transporters in *ephrin-A2* KOs. In addition, we found that dihydrokainate (DHK), a selective GLT-1 inhibitor, reduced glutamate uptake by 17.6% ± 2.4% in wild-type slices and 10.1% ± 4.4% in KO slices (Figure 4C). This result corresponded to approximately 50% less DHK-sensitive uptake in KO slices.

Reduction in glial glutamate transporters has been previously demonstrated to result in an accumulation of extracellular glutamate both in vivo and in vitro (Rothstein et al., 1996). To assess synaptic glutamate concentrations, we performed whole-cell patch-clamp recordings from layer V pyramidal neurons in cortical slices of 1-month-old mice and tested the sensitivity of the evoked excitatory postsynaptic currents (eEPSCs) to L-2-amino-5 phosphonovalerate (L-APV), a low-affinity NMDA receptor antagonist with a fast off rate. The degree of inhibition by L-APV inversely correlates with synaptic glutamate level (e.g., less inhibition by L-APV indicates higher synaptic glutamate concentration) (Choi et al., 2000). We found that the eEPSCs from KO slices were much less sensitive to L-APV (reduced by 31.9% ± 7.1%) than those recorded from wild-type slices (reduced by 58.7% ± 6.3%) (Figure 4D; $p < 0.05$), indicative of an elevated synaptic glutamate level in KO

mice, possibly caused by reduced glial glutamate transport into astrocytes.

Reduction in Glial Glutamate Transport Promotes Spine Elimination

To further investigate the correlation between reduced glial glutamate transport and promoted spine removal in vivo, we treated wild-type mice with DHK, which is permeable to the blood-brain barrier, and followed spine turnover. We found that spine elimination, but not formation, was significantly increased in 1-month-old wild-type mice treated with DHK for 4 days (Figure 4E), a phenotype that resembles the elevated spine loss in *ephrin-A2* KOs. This result suggests that normal glial uptake of glutamate is necessary for maintaining the stability of dendritic spines in the adolescent mouse cortex.

DISCUSSION

During early development, generation of excessive synapses occurs in a constitutive, genetically programmed manner. This initial overproduction of synapses is followed by an experience-dependent pruning process that reduces synaptic connections considerably and leads to maturation of refined neural circuits. While experience is generally believed to be crucial for synapse elimination at this stage, little is known about its underlying molecular mechanisms. In this study, we identify ephrin-A2 as a participant in experience-dependent pruning of cortical synapses. Deficiency of ephrin-A2 selectively promotes experience-induced removal of existing spines, without affecting spine formation or initial stabilization. We further show that ephrin-A2 colocalizes with glial glutamate transporters and regulates synaptic glutamate transmission, suggesting a potential contribution of astrocytes to synaptic pruning during adolescent development.

To date, little is known about the downstream mechanisms of ephrin-A2 regulation of glial glutamate transporters. Ephrin-A2 may be involved in stabilizing glial glutamate transporters at cell membrane by preventing internalization and subsequent degradation. The fact that ephrin-As only contain a GPI-linked domain to anchor them to the membrane makes them depend on other proteins to transduce intracellular signals. Src family protein kinases have been identified as important signaling intermediates downstream of ephrin-As (Davy et al., 1999; Huai and Drescher, 2001; Zimmer et al., 2007). Furthermore, it has been demonstrated that Src kinases participate in regulating expression and maintaining functions of glial glutamate transporters (Koeberle and Bähr, 2008; Rose et al., 2009). The colocalization of ephrin-A2 and glial glutamate transporters also suggests a potential functional crosstalk between ephrin-A2 and glial glutamate transporters that relies on their physical proximity. However, how ephrin-A2 modulates glial glutamate transporters at perisynaptic astrocytic processes needs to be further investigated.

Glutamate transmission and activation of NMDA receptors are involved in both activity-dependent competition and homeostatic regulations—two fundamental mechanisms underlying synaptic plasticity. A critical task of astrocytes in the brain is to remove excess glutamate from the synaptic cleft, thereby ensuring precise synaptic transmission and preventing overactivation of postsynaptic glutamate receptors (Tzingounis and Wadiche, 2007). Thus, reduced glial glutamate uptake in *ephrin-A2* KOs presumably prolongs the effect of synaptic glutamate on postsynaptic NMDA receptors. Enhanced glutamate signaling at active synapses would subsequently augment the imbalance between activate and inactivate synapses, promoting competition-dependent spine elimination via a Hebbian mechanism. Alternatively, a global overactivation of postsynaptic glutamate receptors could trigger homeostatic regulation and lead to a reduction in total synapse number. It is also possible that a combination of these mechanisms contributes to increased spine loss in *ephrin-A2* KOs.

Previous studies have shown that ephrin-A3 is the most abundant ephrin-A ligand in the adult hippocampus and is involved in the morphogenesis of dendritic spines on CA1 pyramidal neurons (Carmona et al., 2009; Murai et al., 2003). Here, we show that ephrin-A2 is more predominant than ephrin-A3 in the cortex and that lack of ephrin-A2, but not ephrin-A3, results in accelerated experience-dependent spine pruning in the adolescent cortex. Moreover, while glial glutamate transporters are upregulated in the hippocampus of *ephrin-A3* KOs (Carmona et al., 2009; Filosa et al., 2009), they are significantly downregulated in the cortex of *ephrin-A2* KOs. Therefore, despite the fact that multiple ephrin-As are functionally redundant in topographic map formation and cortical column integration during early development (Cang et al., 2005; Cutforth et al., 2003; Feldheim et al., 2000; Pfeiffenberger et al., 2005; Torii et al., 2009), our findings suggest that different ephrin-As may regulate synapse morphology and dynamics through distinctive cellular signaling, providing a potential mechanism for achieving the specificity and complexity of mature neuronal networks.

EXPERIMENTAL PROCEDURES

Animals

Thy1-YFP-H line mice (Feng et al., 2000) were purchased from Jackson Laboratory. *Ephrin-A2* and *ephrin-A3* KO mice (Cutforth et al., 2003; Feldheim et al., 2000) were obtained from Dr. David A. Feldheim at UCSC. Wild-type littermates were used as controls and no difference in all analyses was observed between wild-type and heterozygous mice. Sensory deprivation was performed by cutting the mystacial vibrissae of the one side whisker pad to skin level. Sensory enrichment was conducted by housing mice in a standard cage with about 180 strings of beads hanging from the top of the cage, with the string locations changed daily. MK801 (0.25 μg/g body weight) and DHK (10 μg/g body weight) were intraperitoneally injected. Mice were housed and bred in UCSC animal facilities according to approved animal protocol.

In Vivo Transcranial Imaging and Data Quantification

The surgical procedure for transcranial two-photon imaging and data quantification have been described previously (Xu et al., 2009). Percentages of eliminated and formed spines were normalized to total spines counted in the initial image. Spine density was calculated by dividing the number of spines by the length of the dendritic segment. For the spine lifetime analysis, data were fitted with a two-exponential-decay equation using GraphPad Prism: percentage of survival spine = $p_1 \times (1/2)^{t/\tau 1} + p_2 \times (1/2)^{t/\tau 2}$ (p_1 and p_2: proportion of fast- and slow-decay spines, $p_1 + p_2 = 100\%$; τ_1 and τ_2: half-life of fast- and slow-decay spines).

Array Tomography and Data Quantification

Array tomography experiments were performed as previously described (Micheva and Smith, 2007). Briefly, the mouse brain was dissected, fixed,

dehydrated, and embedded in London Resin (LR) White. Serial 70 nm sections were obtained and then probed consecutively with the following primary antibodies: mouse anti-bassoon (1:100; Abcam), mouse anti-SV2 (1:100; DSHB), rabbit anti-synapsin (1:100; Cell Signaling Technology), guinea pig anti-VGluT1 (1:100; Millipore), rabbit anti-PSD95 (1:100; Cell Signaling Technology), mouse-anti-NR1 (1:100; Millipore), mouse anti-GluR2 (1:100; Millipore), rabbit anti-GLAST (1:100), rabbit anti-GLT-1 (1:100), mouse anti-GS (1:100; BD Biosciences), rabbit anti-ephrin-A2 (1:100; Santa Cruz Biotechnology), and goat anti-ephrin-A3 (1:100; Invitrogen). All images were obtained using a Zeiss Axio Imager.Z1 Upright Fluorescence Microscope with motorized stage and Axiocam HR Digital Camera. Image data from sequential sections were computationally aligned, registered, and unwarped. The density of ephrin-As puncta was calculated by dividing puncta numbers by the imaged volume subtracted by the volume of the nuclei. For colocalization analysis, the center of each protein punctum was identified and excitatory synapses were defined using PSD95, SV2, and VGluT1 puncta. Relative distances of ephrin-As centers to other neuronal and astrocytic protein centers within 1 μm from the centers of defined synapses were measured in three dimensions. The numbers of ephrin-As puncta within 100 nm from different protein centers were counted and normalized by total numbers of each protein centers.

Western Blots and Data Quantification

Cortical tissues were dissected and homogenized in ice-cold buffer solution. Denatured lysates were electrophoretically separated by 10% SDS-PAGE and transferred onto nitrocellulose membrane. This was then probed with primary antibodies against GLAST, GLT-1, GS, actin, and tubulin. Western blots were quantified using ImageJ software. Detailed procedures are provided in Supplemental Experimental Procedures.

Glutamate Uptake Assay

Mice (P28–P30) were decapitated and cortical slices (400 μm thick) were prepared in cold artificial cerebrospinal fluid (ACSF) and maintained at room temperature for 1.5–2 hr before stimulation. Cortical slices were incubated for 7 min in ACSF containing 0.5 μCi L-[^{3}H]-glutamate and 100 μM unlabeled glutamate and then rinsed with cold ACSF and homogenized in 1% Triton buffer. The radioactivity of 25 μl lysates was measured and glutamate uptake was normalized to protein concentration. To inhibit glial glutamate transporter-mediated uptake, we incubated cortical slices with 300 μM TFB-TBOA or 500 μM DHK for 30 min prior to uptake measurement.

Cortical Slice Electrophysiology

Coronal slices of the somatosensory cortex were prepared from mice (P28–P30) in ice-cold cutting solution and incubated in ACSF for 30 min at 32°C and 1 hr at room temperature before recording. Whole-cell recordings were made from layer V pyramidal neurons. Synaptic currents were evoked at 0.05 Hz using a concentric bipolar stimulating electrode placed in layer II/III of the same whisker-barrel column. To isolate NMDA receptor currents, we voltage clamped cells at −70 mV and perfused them with an extracellular recording solution lacking Mg^{2+}, in the presence of 10 μM CNQX and 100 μM picrotoxin. To assess concentration of cleft-glutamate, we bath applied 250 μM L-APV in the same Mg^{2+}-lacking solution with 10 μM CNQX and 100 μM picrotoxin. Analysis was done using ClampFit. Detailed procedures are provided in Supplemental Experimental Procedures.

Statistics

p values were calculated using the Student's t test. The numbers of cells/mice analyzed were indicated in the figure.

SUPPLEMENTAL INFORMATION

Supplemental Information includes Supplemental Experimental Procedures and five figures and can be found with this article online at http://dx.doi.org/10.1016/j.neuron.2013.07.014.

ACKNOWLEDGMENTS

We gratefully thank David Feldheim for providing *ephrin-A2* and *ephrin-A3* KO mice; Jeffrey Rothstein for providing GLAST and GLT-1 antibodies; Yi Qin, Ju Lu, and David States for critical comments on the manuscript; Shinya Ito for help with spine lifetime analysis; and Shibo Li, Zhuojun Guo, Maria Ximena Silveyra, Michael Robinson, Benjamin Abrams, Adam Aharon, James Perna, Rebecca Roberts, Andrew Perlik, and Jonathan Zweig for suggestions and assistance with experiments. This work was supported by grants from the National Institute of Mental Health to Y.Z. S.J.S. is a founder of Aratome and chair of its scientific advisory board.

Accepted: July 12, 2013
Published: October 2, 2013

REFERENCES

Aoto, J., and Chen, L. (2007). Bidirectional ephrin/Eph signaling in synaptic functions. Brain Res. *1184*, 72–80.

Bock, J., and Braun, K. (1999). Blockade of N-methyl-D-aspartate receptor activation suppresses learning-induced synaptic elimination. Proc. Natl. Acad. Sci. USA *96*, 2485–2490.

Cahoy, J.D., Emery, B., Kaushal, A., Foo, L.C., Zamanian, J.L., Christopherson, K.S., Xing, Y., Lubischer, J.L., Krieg, P.A., Krupenko, S.A., et al. (2008). A transcriptome database for astrocytes, neurons, and oligodendrocytes: a new resource for understanding brain development and function. J. Neurosci. *28*, 264–278.

Cang, J., Kaneko, M., Yamada, J., Woods, G., Stryker, M.P., and Feldheim, D.A. (2005). Ephrin-as guide the formation of functional maps in the visual cortex. Neuron *48*, 577–589.

Carmona, M.A., Murai, K.K., Wang, L., Roberts, A.J., and Pasquale, E.B. (2009). Glial ephrin-A3 regulates hippocampal dendritic spine morphology and glutamate transport. Proc. Natl. Acad. Sci. USA *106*, 12524–12529.

Changeux, J.P., and Danchin, A. (1976). Selective stabilisation of developing synapses as a mechanism for the specification of neuronal networks. Nature *264*, 705–712.

Chaudhry, F.A., Lehre, K.P., van Lookeren Campagne, M., Ottersen, O.P., Danbolt, N.C., and Storm-Mathisen, J. (1995). Glutamate transporters in glial plasma membranes: highly differentiated localizations revealed by quantitative ultrastructural immunocytochemistry. Neuron *15*, 711–720.

Choi, S., Klingauf, J., and Tsien, R.W. (2000). Postfusional regulation of cleft glutamate concentration during LTP at 'silent synapses'. Nat. Neurosci. *3*, 330–336.

Cutforth, T., Moring, L., Mendelsohn, M., Nemes, A., Shah, N.M., Kim, M.M., Frisén, J., and Axel, R. (2003). Axonal ephrin-As and odorant receptors: coordinate determination of the olfactory sensory map. Cell *114*, 311–322.

Davy, A., Gale, N.W., Murray, E.W., Klinghoffer, R.A., Soriano, P., Feuerstein, C., and Robbins, S.M. (1999). Compartmentalized signaling by GPI-anchored ephrin-A5 requires the Fyn tyrosine kinase to regulate cellular adhesion. Genes Dev. *13*, 3125–3135.

Feldheim, D.A., Kim, Y.I., Bergemann, A.D., Frisén, J., Barbacid, M., and Flanagan, J.G. (2000). Genetic analysis of ephrin-A2 and ephrin-A5 shows their requirement in multiple aspects of retinocollicular mapping. Neuron *25*, 563–574.

Feng, G., Mellor, R.H., Bernstein, M., Keller-Peck, C., Nguyen, Q.T., Wallace, M., Nerbonne, J.M., Lichtman, J.W., and Sanes, J.R. (2000). Imaging neuronal subsets in transgenic mice expressing multiple spectral variants of GFP. Neuron *28*, 41–51.

Filosa, A., Paixão, S., Honsek, S.D., Carmona, M.A., Becker, L., Feddersen, B., Gaitanos, L., Rudhard, Y., Schoepfer, R., Klopstock, T., et al. (2009). Neuron-glia communication via EphA4/ephrin-A3 modulates LTP through glial glutamate transport. Nat. Neurosci. *12*, 1285–1292.

Fu, M., Yu, X., Lu, J., and Zuo, Y. (2012). Repetitive motor learning induces coordinated formation of clustered dendritic spines in vivo. Nature *483*, 92–95.

Hertz, L., and Zielke, H.R. (2004). Astrocytic control of glutamatergic activity: astrocytes as stars of the show. Trends Neurosci. *27*, 735–743.

Holtmaat, A.J., Trachtenberg, J.T., Wilbrecht, L., Shepherd, G.M., Zhang, X., Knott, G.W., and Svoboda, K. (2005). Transient and persistent dendritic spines in the neocortex in vivo. Neuron *45*, 279–291.

Huai, J., and Drescher, U. (2001). An ephrin-A-dependent signaling pathway controls integrin function and is linked to the tyrosine phosphorylation of a 120-kDa protein. J. Biol. Chem. *276*, 6689–6694.

Hubel, D.H., Wiesel, T.N., and LeVay, S. (1977). Plasticity of ocular dominance columns in monkey striate cortex. Philos. Trans. R. Soc. Lond. B Biol. Sci. *278*, 377–409.

Katz, L.C., and Shatz, C.J. (1996). Synaptic activity and the construction of cortical circuits. Science *274*, 1133–1138.

Klein, R. (2009). Bidirectional modulation of synaptic functions by Eph/ephrin signaling. Nat. Neurosci. *12*, 15–20.

Koeberle, P.D., and Bähr, M. (2008). The upregulation of GLAST-1 is an indirect antiapoptotic mechanism of GDNF and neurturin in the adult CNS. Cell Death Differ. *15*, 471–483.

Lai, K.O., and Ip, N.Y. (2009). Synapse development and plasticity: roles of ephrin/Eph receptor signaling. Curr. Opin. Neurobiol. *19*, 275–283.

Lichtman, J.W., and Colman, H. (2000). Synapse elimination and indelible memory. Neuron *25*, 269–278.

Micheva, K.D., Busse, B., Weiler, N.C., O'Rourke, N., and Smith, S.J. (2010). Single-synapse analysis of a diverse synapse population: proteomic imaging methods and markers. Neuron *68*, 639–653.

Micheva, K.D., and Smith, S.J. (2007). Array tomography: a new tool for imaging the molecular architecture and ultrastructure of neural circuits. Neuron *55*, 25–36.

Murai, K.K., Nguyen, L.N., Irie, F., Yamaguchi, Y., and Pasquale, E.B. (2003). Control of hippocampal dendritic spine morphology through ephrin-A3/EphA4 signaling. Nat. Neurosci. *6*, 153–160.

Murai, K.K., and Pasquale, E.B. (2004). Eph receptors, ephrins, and synaptic function. Neuroscientist *10*, 304–314.

Nicoll, R.A., and Malenka, R.C. (1999). Expression mechanisms underlying NMDA receptor-dependent long-term potentiation. Ann. N Y Acad. Sci. *868*, 515–525.

Nimchinsky, E.A., Sabatini, B.L., and Svoboda, K. (2002). Structure and function of dendritic spines. Annu. Rev. Physiol. *64*, 313–353.

Pfeiffenberger, C., Cutforth, T., Woods, G., Yamada, J., Rentería, R.C., Copenhagen, D.R., Flanagan, J.G., and Feldheim, D.A. (2005). Ephrin-As and neural activity are required for eye-specific patterning during retinogeniculate mapping. Nat. Neurosci. *8*, 1022–1027.

Rose, E.M., Koo, J.C., Antflick, J.E., Ahmed, S.M., Angers, S., and Hampson, D.R. (2009). Glutamate transporter coupling to Na,K-ATPase. J. Neurosci. *29*, 8143–8155.

Rothstein, J.D., Dykes-Hoberg, M., Pardo, C.A., Bristol, L.A., Jin, L., Kuncl, R.W., Kanai, Y., Hediger, M.A., Wang, Y., Schielke, J.P., and Welty, D.F. (1996). Knockout of glutamate transporters reveals a major role for astroglial transport in excitotoxicity and clearance of glutamate. Neuron *16*, 675–686.

Sawtell, N.B., Frenkel, M.Y., Philpot, B.D., Nakazawa, K., Tonegawa, S., and Bear, M.F. (2003). NMDA receptor-dependent ocular dominance plasticity in adult visual cortex. Neuron *38*, 977–985.

Segal, M. (2005). Dendritic spines and long-term plasticity. Nat. Rev. Neurosci. *6*, 277–284.

Sin, W.C., Haas, K., Ruthazer, E.S., and Cline, H.T. (2002). Dendrite growth increased by visual activity requires NMDA receptor and Rho GTPases. Nature *419*, 475–480.

Tada, T., and Sheng, M. (2006). Molecular mechanisms of dendritic spine morphogenesis. Curr. Opin. Neurobiol. *16*, 95–101.

Torii, M., Hashimoto-Torii, K., Levitt, P., and Rakic, P. (2009). Integration of neuronal clones in the radial cortical columns by EphA and ephrin-A signalling. Nature *461*, 524–528.

Tzingounis, A.V., and Wadiche, J.I. (2007). Glutamate transporters: confining runaway excitation by shaping synaptic transmission. Nat. Rev. Neurosci. *8*, 935–947.

Xu, T., Yu, X., Perlik, A.J., Tobin, W.F., Zweig, J.A., Tennant, K., Jones, T., and Zuo, Y. (2009). Rapid formation and selective stabilization of synapses for enduring motor memories. Nature *462*, 915–919.

Yang, G., Pan, F., and Gan, W.B. (2009). Stably maintained dendritic spines are associated with lifelong memories. Nature *462*, 920–924.

Yuste, R., and Bonhoeffer, T. (2001). Morphological changes in dendritic spines associated with long-term synaptic plasticity. Annu. Rev. Neurosci. *24*, 1071–1089.

Zimmer, G., Kästner, B., Weth, F., and Bolz, J. (2007). Multiple effects of ephrin-A5 on cortical neurons are mediated by SRC family kinases. J. Neurosci. *27*, 5643–5653.

Zuo, Y., Lin, A., Chang, P., and Gan, W.B. (2005a). Development of long-term dendritic spine stability in diverse regions of cerebral cortex. Neuron *46*, 181–189.

Zuo, Y., Yang, G., Kwon, E., and Gan, W.B. (2005b). Long-term sensory deprivation prevents dendritic spine loss in primary somatosensory cortex. Nature *436*, 261–265.